

Development of Manganese Build-up Resistant Cermet Coatings for Hearth Rolls

CHENG-SHENG YU*, TSAI-SHANG HUANG**, JING-YI HUANG*
and MAO-JENG TSENG***

*New Materials Research & Development Department

**Iron and Steel Research & Development Department

*** Plant Engineering & Maintenance Department
China Steel Corporation

Agglomerate sintered NiCrAlY-Y₂O₃ cermets were prepared from NiCrAlY alloy and Y₂O₃ powders. To obtain the coatings, agglomerate sintered NiCrAlY- Y₂O₃ cermets and three commercially available cermets, CoCrAlY-Y₂O₃-CrB₂, CoNiCrAlYZr-Cr₃C₂-ZrB₂, and CoNiCrAlY-Cr₃C₂-Y₂O₃, were thermally sprayed onto stainless steel substrates using a High Velocity Oxygen Fuel (HVOF) sprayer. These four thermally sprayed coatings' build-up resistances were comparatively evaluated by contacting them with MnO powders and manganese-containing carbon steel. After the reactions were completed, the surface roughness and Mn concentration of the coatings were examined. With a lower Cr concentration in the alloy and the absence of Cr-containing carbide or boride in the cermets, the NiCrAlY-Y₂O₃ cermet coating had the best manganese build-up resistance.

Keywords: Mn Build-up, Cermets, NiCrAlY super-alloy, Hearth roll, HVOF

1. INTRODUCTION

In a continuous annealing furnace, hearth rolls for carrying steel sheets need to possess high wear, build-up and thermal shock resistant coatings. A major problem encountered in the annealing operation is the transfer or build-up of material from the steel sheet to the hearth rolls. If build-up occurs, it will accumulate on the hearth rolls and damage the steel sheet that is being processed. The build-up may stem from a reaction of the coating on the rolls with the iron oxide or manganese oxide on the steel surface. This problem has become more critical since higher processing speeds were introduced to increase the productivity of high strength manganese-containing steels. Therefore, different compositions of coating materials for hearth rolls have been developed in the past decades to promote build-up resistance⁽¹⁻⁶⁾. One of the special iron build-up resistant cermets using multiple metal components, such as Co, Cr, Ta, Al, Si, and Y, to form the alloy and blended with wear-resistant aluminum oxides were developed and designated as LCO-17^(5,6). This blended cermet powder could then be thermally sprayed by plasma and detonation gun spray systems, while it is not recommended to use a High Velocity Oxygen Fuel (HVOF) spraying system due to the lower temperature in the flame and

the lower flow ability⁽⁷⁾.

However, when HVOF became the main thermal spray system, agglomerate sintered cermet powders needed to be developed to replace the blended type. Because the manganese on the surface of steel sheet could react with the aluminum oxide in the LCO-17 coating, new cermets with a higher manganese build-up resistance needed to be researched. Special compositions of MCrAlY super alloy, Y₂O₃, CeO₂, MgO, ZrO₂ based ceramics, and some carbides and borides, were the candidate components for these new cermets⁽¹⁻⁴⁾. In this study, we prepared agglomerate sintered NiCrAlY-Y₂O₃ cermet powder through the spray drying and sintering process route. The agglomerate sintered NiCrAlY-Y₂O₃ cermet powder and three commercially available cermet powders CoCrAlY-Y₂O₃-CrB₂, CoNiCrAlYZr-Cr₃C₂-ZrB₂, and CoNiCrAlY-Cr₃C₂- Y₂O₃, were thermally HVOF sprayed onto stainless steel substrates to prepare the coated specimens to evaluate manganese build-up resistance.

2. EXPERIMENTAL

The agglomerate sintered NiCrAlY-Y₂O₃ cermet powders were produced using NiCrAlY powder with sizes below 20μm and fine yttria powder with an average size of about 3μm as the starting raw materials

as shown in Figs.1(a) and (b). The chemical composition of the NiCrAlY powder supplied by TTMC Ltd is Ni-17Cr-4.5Al-0.3Y, and the purity of the yttria used is 99.95%. The suspension for spray drying was prepared by mixing 90% alloy and 10% yttria powders, PVA binder and water, and stirring for at least 15 min. The suspension was dried by a rotary disk type spray-dryer to form granules. The agglomerate powder was sintered at a temperature above 1200°C for more than 4 hrs in a reducing atmosphere as shown in Fig.2. The agglomerate sintered NiCrAlY-Y₂O₃ cermet powder was HVOF sprayed on flat SUS 316 substrates with dimensions of L×W×H = 25×25×8mm. The substrates were grit-blasted before the thermal spraying. A Sulzer Metco Diamond Jet DJ2700 HVOF thermal spray system using propylene fuel was employed to develop the coatings. The spraying distance was 230 mm, and the feeding rate of the cermet powder was 38 g/min. The propylene fuel and oxygen were at a pressure of 0.76 and 1.05 MPa, respectively. The coatings made from NiCrAlY-Y₂O₃, CoCrAlY-Y₂O₃-CrB₂, CoNiCrAlY-Zr-Cr₃C₂-ZrB₂, and CoNiCrAlY-Cr₃C₂-Y₂O₃ cermet coatings were designated as AS-MY10, HG-3, TS-1, and TS-4, respectively. These coatings were characterized by using a scanning electron microscope (SEM), energy dispersive spectroscopy (EDS), X-ray mapping, and X-ray diffraction.

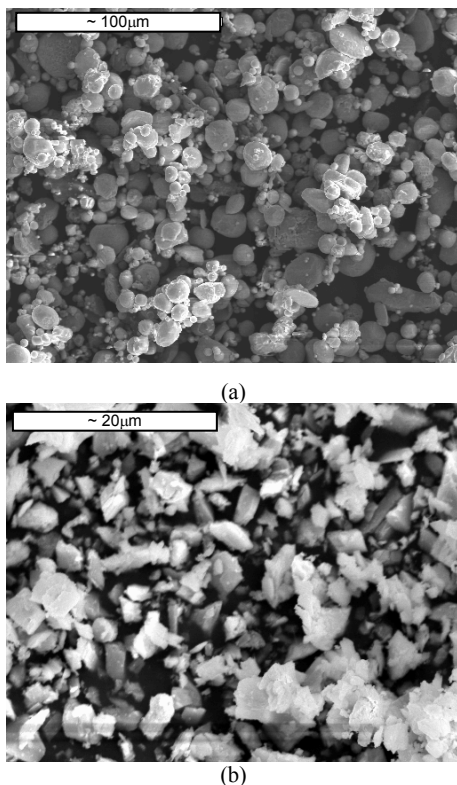


Fig.1. SEM micrographs of fine (a) NiCrAlY super alloy powder, and (b) yttria powder.

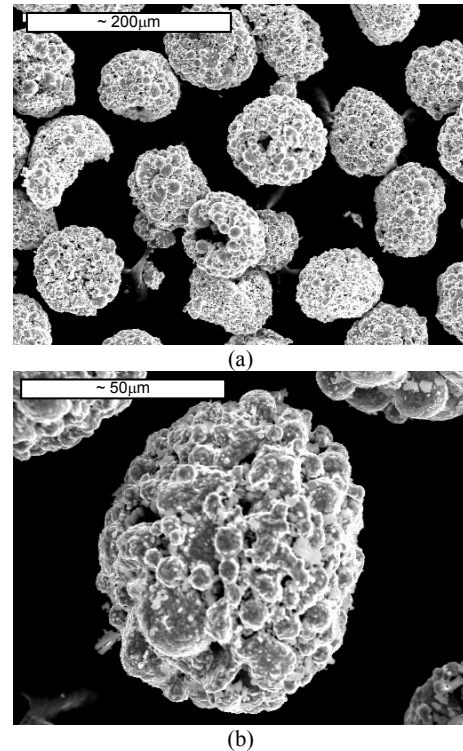


Fig.2. SEM micrographs of (a) agglomerate sintered, and (b) single granular 90NiCrAlY-10Y₂O₃ cermet powder (MY10).

The specimens used for evaluating build-up resistance were established by putting manganese-containing steel or manganese oxide (MnO) powders in between two coated substrates. Before build-up resistance testing, the surface roughness (Ra) of the coatings was polished to 0.2 μm. The composition of manganese-containing steel is Fe-1.25Mn-1Cr-0.22Si-0.5C, and the purity of MnO is 99%. The thickness of the powders or steels between the two coated substrates is more than 2 mm. The sandwich-like specimens were put into a furnace with a nitrogen and 5% hydrogen atmosphere and held at a temperature of 950°C for 100 hrs. After the continuous contacting reaction, the top surface and a cross section of the coatings were examined by SEM-EDS analysis. From the residues that remained on the surface, the surface roughness and Mn content were measured to evaluate the build-up resistance of the coatings⁽³⁾. The porosity of the coatings was measured from the cross sectional SEM micrographs using image analysis software according to ASTM E562.

3. RESULTS AND DISCUSSION

3.1 Characterization of coatings

The SEM micrographs and corresponding EDS analyses of the four coatings are shown in Fig.3.

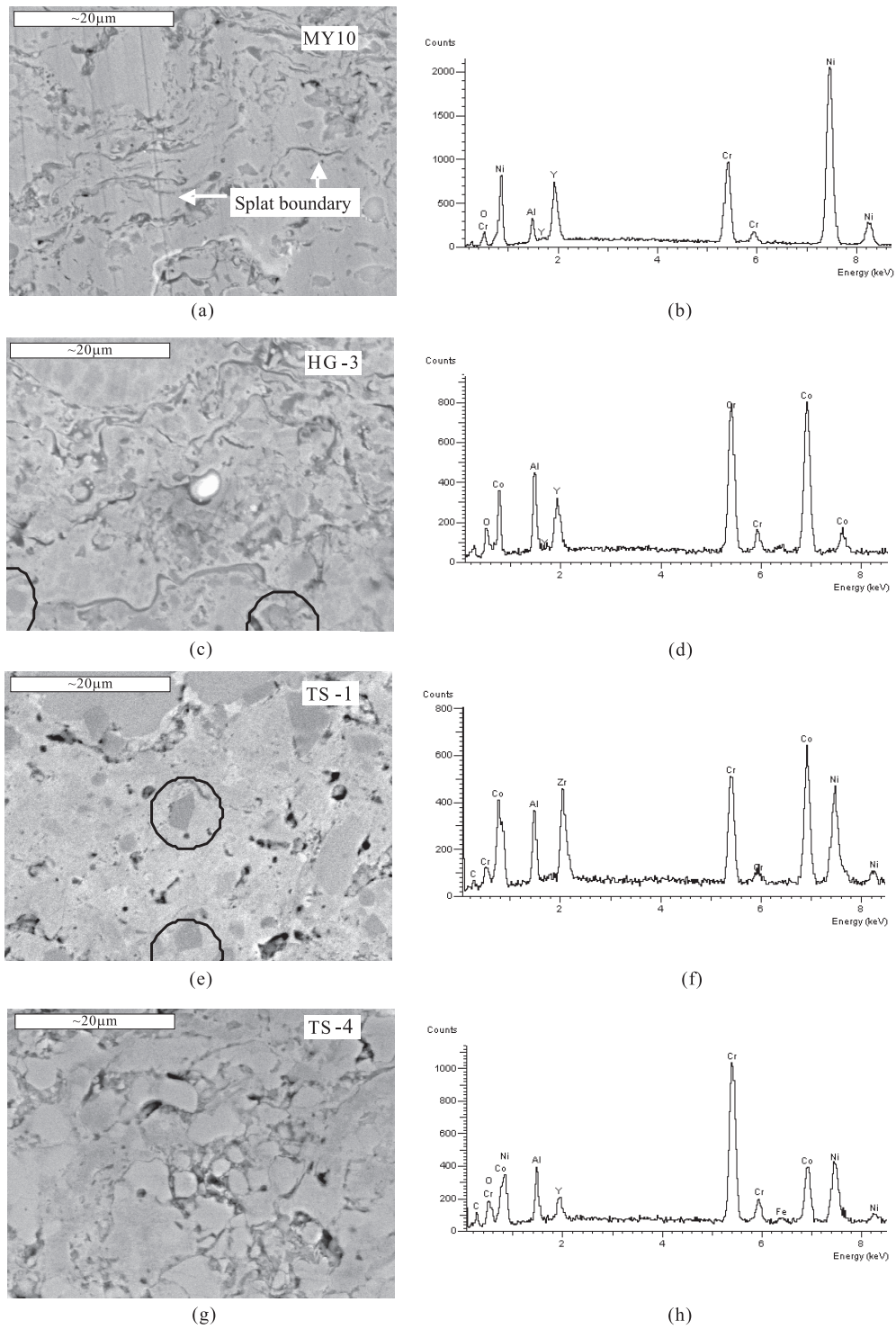


Fig.3. SEM micrographs of cross sectional and typical compositions analyzed by EDS for (a) and (b) MY10, (c) and (d) HG-3, (e) and (f) TS-1, (g) and (h) TS-4 coatings.

Figures 3(a), (c), (e), and (g) show the cross sectional micrographs, while Figures 3(b), (d), (f), and (h) show the energy-dispersive spectra of the MY10, HG-3, TS-1, and TS-4 cermet coatings, respectively. As

shown in Fig.3(a), the splat boundaries exist in the MY10 coating and the HG-3 coating. By comparing the pore morphologies of these four coatings, more pores are exhibited in TS-1 and TS-4 coatings. The porosity

measured from the cross sectional MY10, HG-3, TS-1 and TS-4 coatings are 0.9 ± 0.5 , 0.6 ± 0.2 , 2.2 ± 1.6 and $2.8 \pm 1.56\%$, respectively. Some dark particles in the HG-3 and TS-1 coatings are attributed to the presence of borides such as CrB_2 or ZrB_2 in the cermet powders. The EDS analyses in Fig. 3 shows that the Cr content is relatively high for the HG-3 and TS-4 coatings. The high Cr content in the HG-3 cermet coatings comes from the cermet powders containing chromium boride and CoCrAlY super alloy with a high Cr concentration. The high Cr contents in the TS-4 coatings may stem from the 30~50% chromium carbide added in the cermet powders⁽⁸⁾. Zirconium, as opposed to yttrium, is one of the major elements in the TS-1 cermet coating, and it may imply that the super alloy in the TS-1 cermet coating is CoNiCrAlYZr instead of the conventional super alloy CoNiCrAlY .

The typical elemental compositions of these four coatings are shown in Table 1. The Al contents in the four coatings are similar, ranging from about 2 to 4%, while Cr contents are quite different, ranging from 14 to 41%. The compositions of the alloys of MY10 and

HG-3 coatings are different, one is NiCrAlY while the other is CoCrAlY , but both have the yttrium oxide added. According to the claims of the supplier⁽¹⁾, HG-3 cermet coatings contain a CrB_2 component, and this is one of the reasons why the Cr content in HG-3 is more than it is in MY10 coatings. The contributions of Cr in HG-3 are partly from alloy and chromium boride. The boron in HG-3 coating could not be detected by SEM-EDS but has been observed by the mapping of EPMA. As shown in Table 1, TS-1 and TS-4 coatings both contain the carbon element, and this is due to the chromium carbide that had been added into both cermet powders. The TS-4 coating not only contains chromium carbide but also yttria as claimed by its supplier⁽⁸⁾, and the yttrium and oxygen were both detected by EDS in Table 1. The MY10 coating has the least Cr content as compared to that of the other coatings.

3.2 Build-up resistance of coatings

Figure 4 shows the appearances of MY10, HG-3, TS-1 and TS-4 coatings after contacted reaction with

Table 1 Typical EDS analyses of cross sectional MY10, HG-3, TS-1, TS-4 coatings

Coatings	Element (%)							
	C	O	Al	Cr	Co	Ni	Y	Zr
MY10		1.21	2.67	14.67	--	67.86	13.59	--
HG-3		3.24	3.91	33.22	52.58	--	7.05	
TS-1	6.88	--	2.04	22.66	32.31	26.30		9.81
TS-4	1.04	1.02	2.63	41.68	21.54	28.74	3.00	--

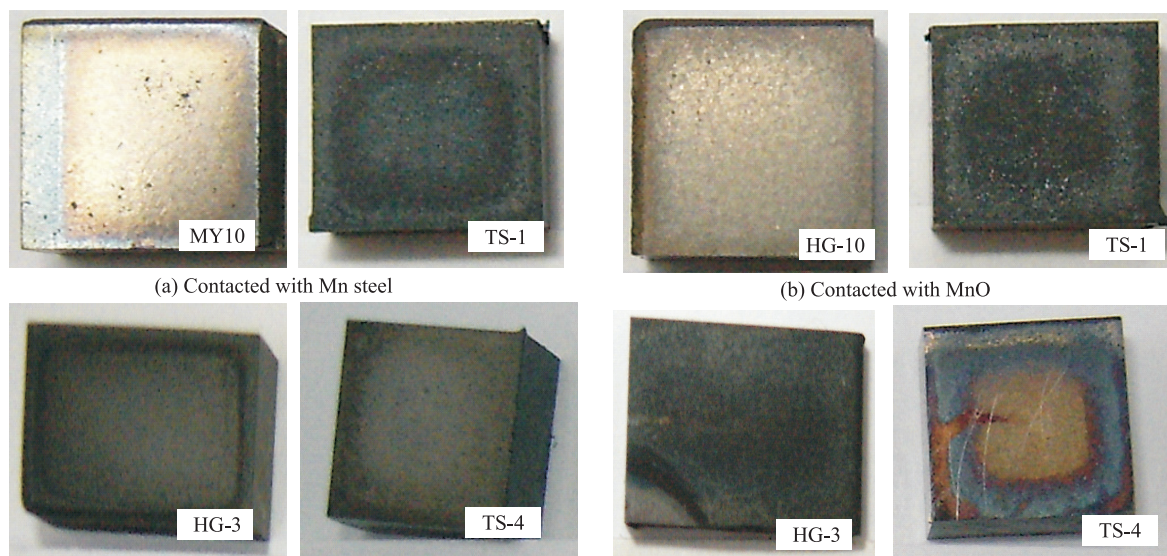


Fig.4. Photographs of MY10, HG-3, TS-1, TS-4 coatings after contacted reaction with (a)Mn bearing steel, (b)MnO at 950°C in $\text{N}_2 + 5\%\text{H}_2$ for 100 hrs.

Mn bearing steel plate and MnO powders, respectively. From photographs shown as Figs.4(a) and 4(b), it is evident that the residues of Mn bearing steel and MnO did not stick on all coatings, but an obvious color change occurred on the surfaces of HG-3, TS-1 and TS-4 coatings. After exposure to Mn bearing steel, all the coatings showed different small levels of damage. However, after exposure to MnO, the HG-3, TS-1, and TS-4 coatings all revealed obvious damage. The Mn content, Fe content, and surface roughness (Ra) of the four coatings after contact reaction with Mn bearing steel and MnO at 950°C in N₂ and 5%H₂ for 100 hrs are shown in Table 2. Surface roughness after reaction

could be used to judge the degree of reaction and the amount of build-ups on the surface of the coatings⁽³⁾. As also shown in Table 2, after exposure to Mn bearing steel, TS-4 coating's surface had the highest Mn content of 1.7±0.3%, and MY10 had the highest Fe content of 2.7±1.4%. After exposure to MnO, the MY10 coating has the lowest Mn content of 15.1±0.6%, and coatings containing Boride such as HG-3, or Carbide such as TS-1 and TS-4 coatings have higher Mn contents of 33.5±8.8%, 64.8±1.5% and 46.2±0.9%, respectively. The TS-1 coating composed of ZrB₂ and Cr₃C₂ had the highest Mn content. The SEM-line scan analysis of TS-1 and HG-3 coatings after reaction with

Table 2 The Mn, Fe contents and surface roughness of MY10, HG-3, TS-1, TS-4 coatings after contact reaction with Mn bearing steel and MnO at 950°C in N₂ and 5%H₂ for 100 hrs

Coating	Composition	After reaction with Mn bearing steel			After reaction with MnO		
		Mn(%)	Fe(%)	Ra(μm)	Mn(%)	Fe(%)	Ra(μm)
MY10	NiCrAlY+ Y ₂ O ₃	0.4±0.3	2.7±1.4	1.15±0.16	15.1±0.6	5.4±1.1	0.86±0.11
HG-3	CoCrAlY+ CrB ₂ + Y ₂ O ₃	0.2±0.2	1.3±0.2	0.98±0.02	33.5±8.8	0.5±0.5	2.15±0.23
TS-1	CoNiCrAlY+ Cr ₃ C ₂ +ZrB ₂	0.2±0.2	1.4±0.4	1.85±0.03	64.8±1.5	9.2±1.9	3.18±0.81
TS-4	CoNiCrAlY+ Cr ₃ C ₂ + Y ₂ O ₃	1.7±0.3	1.5±0.6	1.43±0.39	46.2±0.9	17.4±1	1.92±0.14

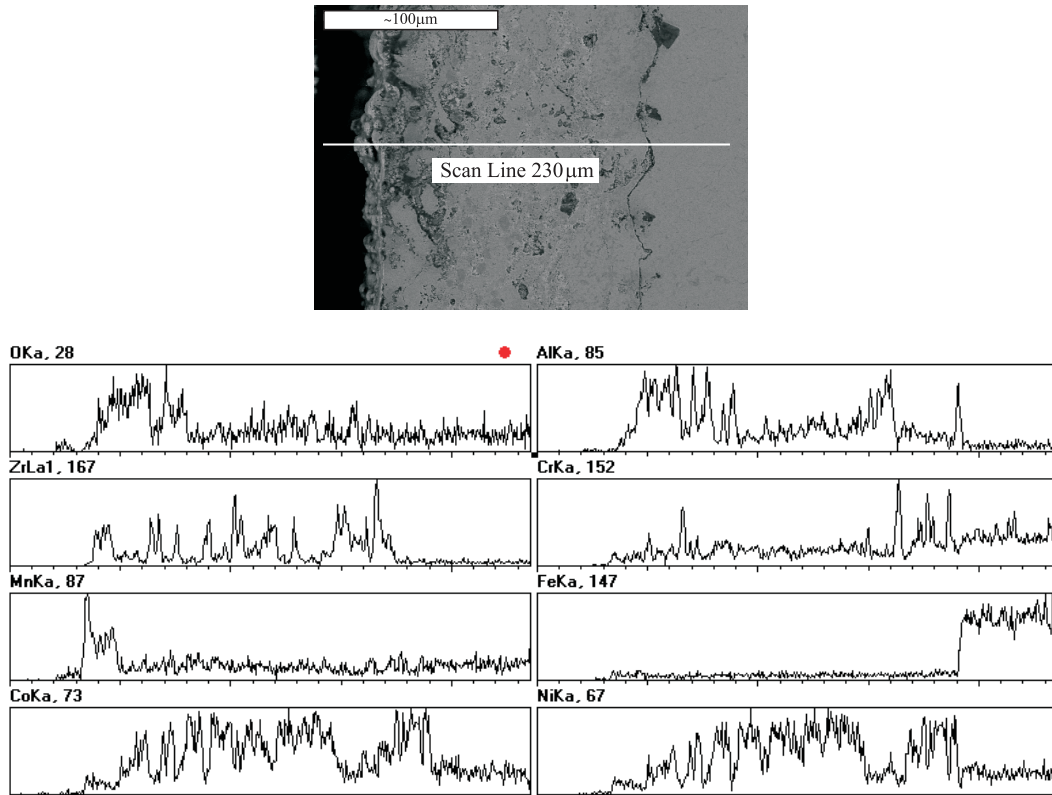


Fig.5. SEM-line scan analysis of TS-1 coating after reaction with MnO.

MnO are shown in Figs.5 and 6. After the TS-1 coating reacted with MnO, the elements of Mn, Al, Zr, and O were seen 25 μ m deep into the coating, with apparent Al rich in the reaction layer. That the enriched elements of O, Mn, Al, and Zr appear at the same location in the line scan seems to imply that the addition of ZrB₂ in the coating allows the Al and Zr in the alloy and zirconium boride to oxidize and form Mn(AlZr)_xO_y. In Figure 6, the line scan analysis of the HG-3 coating after reaction with MnO shows the elements of Mn, Al, Cr, O, and Co at the same location 30 μ m deep into the coating, but with Y and Mn separated. The HG-3 coating may be reacting with

the MnO to form Mn(AlCrCo)_xO_y. The posited reaction would induce the elements of O, Mn, Al, Cr, and Co to form in a concentrated area of the coating. However, the Mn is only on the coating surface, and no apparent Mn exists deeper into the coating.

As shown in Fig.7, after MY10 coating reacted with Mn bearing steel, the surface contained several particles, and these particles are believed to be the origin of the formation of build-ups. The EDS analysis shown in Fig.7(b) indicated that the particles are mostly composed of Cr and N, with few containing Fe and Mn. The X-ray diffraction pattern of AS-MY10 coating after contact reaction with Mn bearing steel is shown in

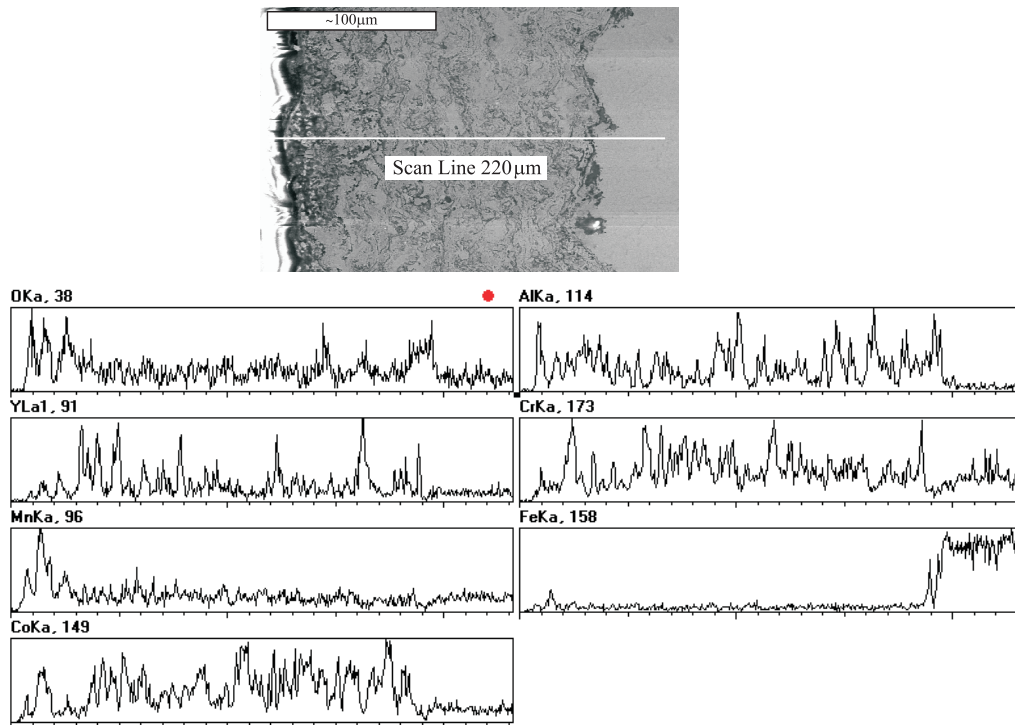


Fig.6. SEM-line scan analysis of HG-3 coating after reaction with MnO.

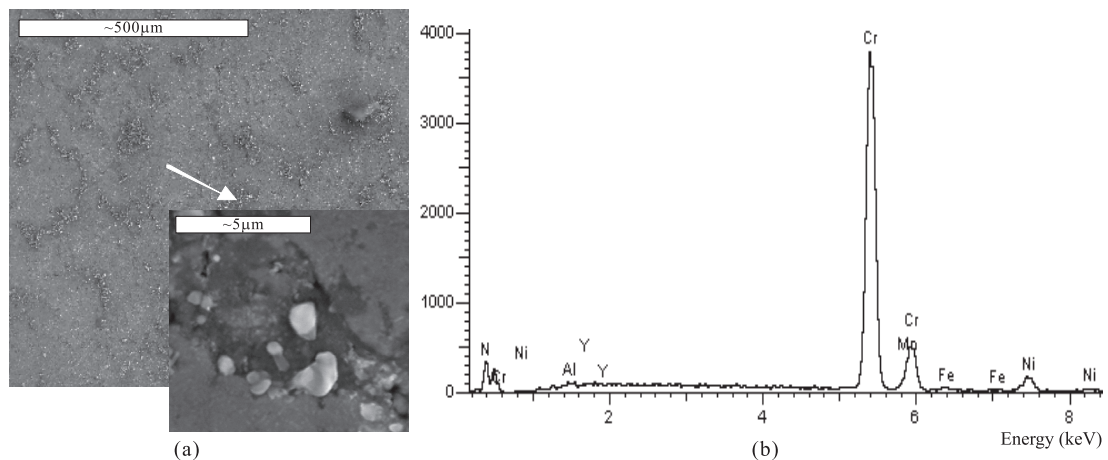


Fig.7. (a)Surface morphologies and (b)EDS analysis of particle on surface of MY10 coating after contacted reaction with Mn bearing steel.

Fig.8. The reaction products found on the surface were γ -CrN (at diffraction angle $2\theta = 37.5, 43.5, 63.5^\circ$). From the analyses of Fig.7(b) and Fig. 8, it is indicated the particles formed on the surface is γ -CrN.

Actually, in the reducing atmosphere, it is hard to find the oxides on the surface of the coating which contacts steel as described by Bi⁽⁹⁾, such as the spinels of $Mn_{1.5}Cr_{1.5}O_4$ and $MnAl_2O_4$, formed by the intentional oxidation of CoCrAlY-CrB₂ coating in air. However, when MY10 coating reacted with manganese oxide, the $MnCr_2O_4$ is formed on the surface as shown in Fig.9. XRD analysis of MY10 coating after reaction with MnO shows that γ -CrN and $MnCr_2O_4$ coexist in the coating. This may be caused by the formation of γ -CrN first which then reacts with MnO to form $MnCr_2O_4$.

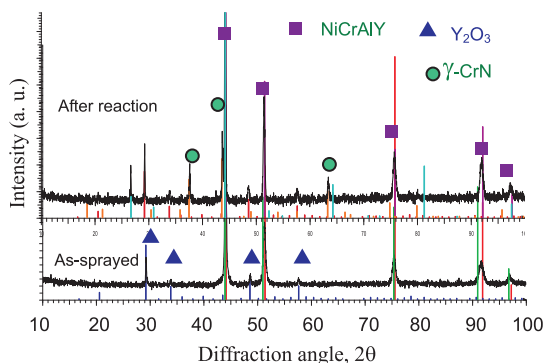


Fig.8. X-ray diffraction patterns of MY10 coating before and after contacted reaction with Mn bearing steel.

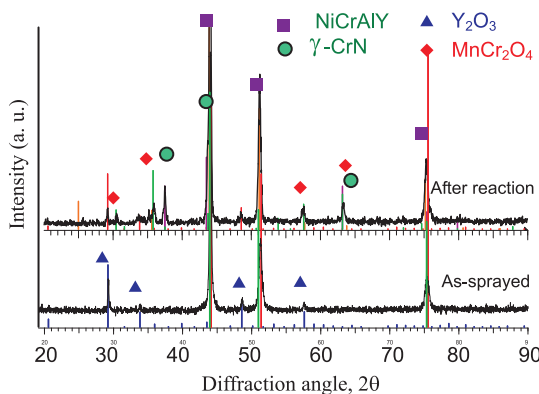


Fig.9. X-ray diffraction patterns of MY10 coating before and after contacted reaction with MnO.

The morphology and X-ray mapping of the reaction marks (dark grey color) of cross sectional MY10 coating after contact reaction with MnO is shown in Fig.10. The reaction marks are rich in O, Al, Y, and Cr, but lack Mn, Fe, and Ni. The depletion

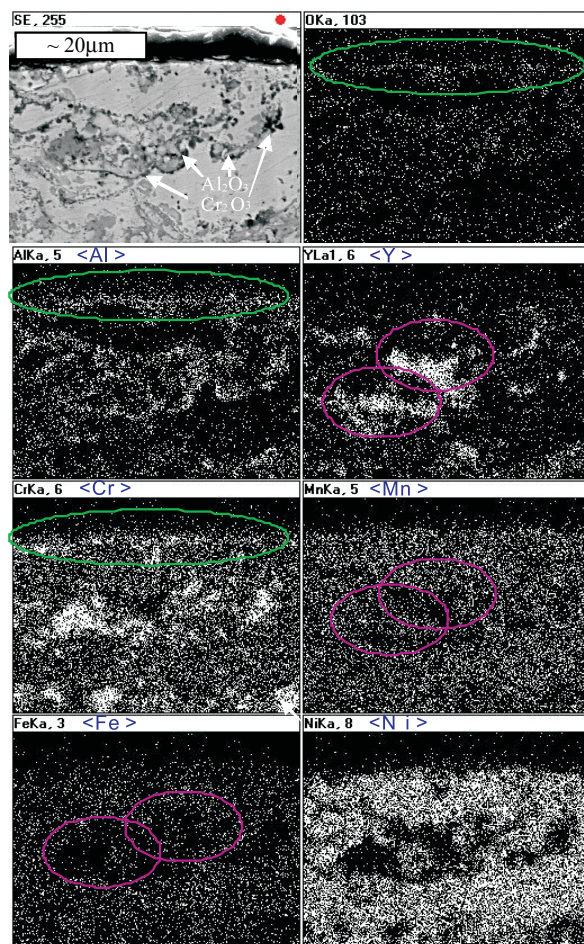


Fig.10. X-ray mapping of O, Al, Y, Cr, Mn, Fe and Ni in reaction mark area of cross sectional MY10 coating after contacted reaction with MnO.

of Fe and Mn is especially apparent in the Y rich areas of the coating. This indicates that the Y_2O_3 act as a diffusion barrier to the reaction species of Mn and Fe. But around the yttria (Y_2O_3), concentrated Al and Cr accompanied by enriched oxygen are noticed in Fig.10. It indicated that wherever the reaction species from MnO is retarded around yttria, the oxidation of Al and Cr in NiCrAlY splat appears. The oxides formed along the splat boundaries and pores have been reported as Cr_2O_3 and Al_2O_3 streaks by Mahesh et al.⁽¹⁰⁾ after NiCrAlY-CeO₂ coating is oxidized in air at 900°C and that they have the function of decreasing further oxidation. The added yttria in cermet splats and the formation of streak like oxides during reaction are acting as diffusion barriers in the contact reaction of MY10 coating and MnO. This illustrated that MY10 coating could have a better performance of manganese oxide build-up resistance. Table 2 shows that the surface roughness directly reflects build-up resistance in the coating. The surface roughness Ra is least

when MY10 is exposed to MnO. The surface roughness measurements are consistent with the EDS results, as coatings with more Mn and Fe have higher surface roughness.

Figure 11 shows TS-1 and HG-3 cermet coated hearth rolls after serving in the continuous annealing line (CAL) or continuous galvanizing line (CGL) line in China Steel (CSC). A hearth roll with TS-1 coating after serving 14 months is shown in Fig.11(a), where build-ups were formed and the coating started to peel off. As evidenced in this research, the zirconium boride engaged in build-up reaction to form $Mn(AlZr)_xO_y$, and the hard polygonal boride particles were oxidized and softened causing the scale off. A hearth roll with HG-3 coating is shown in Fig.11(b) after serving 2 and 20 months. The build-ups with maroon color were formed after the short operation

period of 2 months. The EDS analysis shows that Mn, Al, Cr and O are the major compositions in the build-ups, which is consistent with the observation that the HG-3 coatings that contacted with MnO form $Mn(AlCrCo)_xO_y$ build-up on the surface of the coatings. Although MY10 has a better Mn build-up resistance, a coating employed for hearth rolls needs to have a better hardness. The absence of hard phases, such as CrB_2 , ZrB_2 and Cr_3C_2 , in the MY10 coating may not be good enough for service.

4. CONCLUSIONS

The manganese build-up resistance behavior of HVOF sprayed agglomerate sintered $NiCrAlY-Y_2O_3$ cermet coatings and three commercial cermet coatings have been studied. The following conclusions are made:

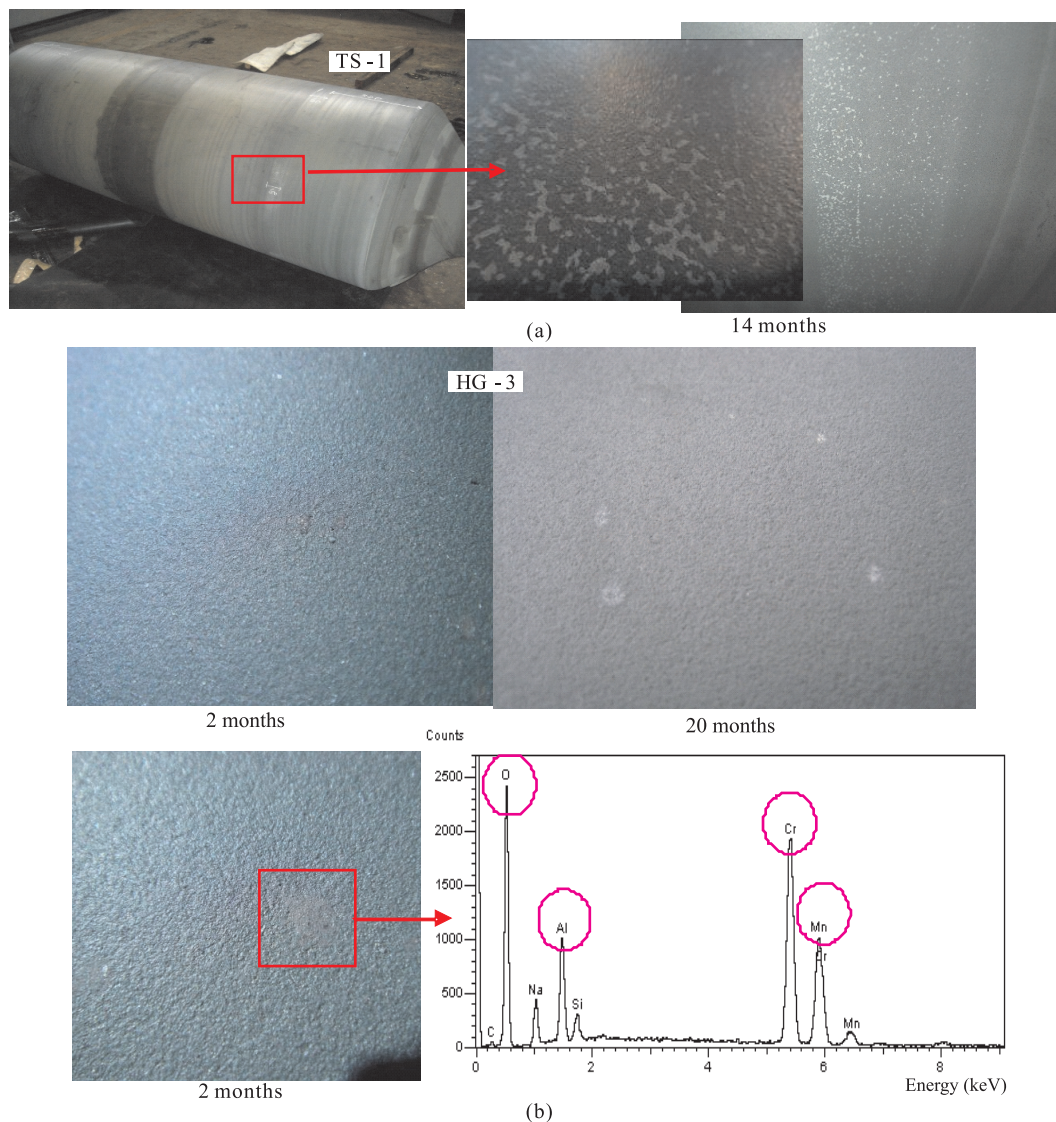


Fig.11. Hearth rolls with (a)TS-1 coating after served 14 months and (b)HG-3 coating after served 2 or 20 months.

1. A hightemperature hearth roll uses super alloy CoNiCrAlY, carbide, boride, and oxide to form cermet powder, where adjusting the amount of Cr and Al in the super alloy and additional oxides is the key to minimizing manganese build-up.
2. Comparing the newly developed agglomerate sintered cermet powder MY10 (Ni-17Cr-4.5Al-0.3Y+10%Y₂O₃) with commercial HG-3 (CoCrAlY+CrB₂+Y₂O₃), TS-1 (CoNiCrAlYZr+Cr₃C₂+ZrB₂), and TS-4(CoNiCrAlY+Cr₃C₂+Y₂O₃), MY10 has the best anti-Mn build-up ability, as the Mn contents in the coating after reaction with MnO are 15.1±0.6%, 33.5±8.8%, 64.8±1.5%, and 46.2±0.9% respectively. These results are also consistent with the measurements of surface roughness Ra.
3. The coating on the hearth roll is composed of a super alloy containing Cr, which easily forms particles of CrN in a N₂ atmosphere. It then forms MnCr_xO_y, which is when the build-up begins to form. Thus, coatings that contain Cr, CrB₂, or Cr₃C₂ inevitably increase Mn build-up.
4. Yttrium oxides in the agglomerate sintered MY10 cermet coatings are passive to manganese oxide. Cr and Al around the sides of yttrium oxide can be easily oxidized to act as barriers to limit Mn diffusion species from forming Mn(Al,Cr)_xO_y in the coating, achieving the goal of preventing Mn build-ups.

REFERENCES

1. I. Yoshitaka, O. Junji, S. Nobuharu, K. Nobuhiko and K. Koji: "Thermal spray material and its coated article excellent in high-temperature wear resistance and build-up resistance", EP0440437, Jan. 30 (1991).
2. J. E. Jackson, H. Nitta, K. Shoichi, M. Amano, Y. Kurisu, and K. Ohno: "Process for Forming A Refractory Oxide Coating", U. S. Patent 5418015, Praxair, May 23 (1995).
3. Yang Gan and Saitama-ken: "Hearth Roll with Superior Endurance Capacity", U. S. Patent 5700423, Dec. 23 (1997).
4. S. Midorikawa and S. Katoh: "Cermet Powder for Sprayed Coating Excellent in build-up Resistance and Roll Having Sprayed Coating Thereon", U. S. Patent 6572518, Jun. 3 (2003).
5. T. A. Wolfla and R. C. Tucker: "High Temperature Wear Resistant Coating Composition", U. S. Patent 4124737, Nov. 7 (1978).
6. H. H. Fukubayashi, K. T. Hiroshima, R. C. Tucker and T. A. Taylor: "High Volume Fraction Refractory Oxide, Thermal Shock Resistant Coatings", U. S. Patent 4822689, Apr. 18 (1989).
7. K. Tsushima: "Coatings for furnace rolls in steel processing", Praxair surface technologies, (2011).
8. K. Akira and M. Kazuo: "Thermal Spraying Powder, Thermal Spray Coating, and Hearth Roll", TW200916603A, March. 26 (2008).
9. Bi Gang: "Research on Influence of Oxygen on CrB₂/CoCrAlY Hearth Roll Coating", The Third Baosteel Biennial Academic Conference 2008, J-201-J-205.
10. R. A. Mahesh, R. Jayaganthan and S. Prakash: "A Study on the Oxidation Behavior of HVOF Sprayed NiCrAlY-0.4wt% CeO₂ Coatings on Superalloys at Elevated Temperature", Materials Chemistry and Physics, 119 (2010), pp. 449-457. □